Experimental investigation of the fire extinguishing capability of ferrocene-containing water mist

Yusuke Koshiba [a,*], Shinji Okazaki [a], and Hideo Ohtani [b]

[a] Department of Materials Science and Chemical Engineering, Faculty of Engineering, Yokohama National University, 79-5 Tokiwadai, Hodogaya-ku, Yokohama 240-8501, Japan

[b] Department of Safety Management, Faculty of Environmental and Information Sciences, Yokohama National University, 79-7 Tokiwadai, Hodogaya-ku, Yokohama 240-8501, Japan

* Corresponding author: Telephone number: +81 45 339 3985

Fax number: +81 45 339 3985

E-mail address: ykoshiba@ynu.ac.jp

Complete postal address: 79-5 Tokiwadai, Hodogaya-ku, Yokohama 240-8501, Japan

Abstract

This study focuses on the fire-suppression capabilities and corrosive properties of ferrocene dispersions. The motivation behind the present study was to develop a high-performance, phosphorus-free fire suppressant. Aqueous dispersions containing micron-sized ferrocene particles and surfactants were prepared using sonication techniques. In this study, Triton X-100 (TX), Noigen TDS-80 (NT), Tween 60 (T60), and Tween 80 (T80) were used as surfactants. Suppression experiments involving pool fires clearly indicated that aqueous ferrocene dispersions containing TX and micron-sized ferrocene with a d_{50} = 16.9 micron exhibit shorter extinguishing times than a conventional wet chemical. Corrosion trials using steel plates immersed in ferrocene dispersions containing TX confirmed that there was no pitting corrosion, implying that ferrocene dispersions containing TX do not present a corrosion risk.

1. Introduction

As shown in Fig. 1, the fire statistics of Japan indicate that the number of deaths and the economic losses due to fires were 1,678 and approximately 85.3 billion yen, respectively, in 2014 [1]. Developing a more effective fire suppressant can make a large contribution to containing fires and reducing casualties and economic losses caused by such fires. Ammonium dihydrogen phosphate ($NH_4H_2PO_4$) is an active substance in ABC powder, which is widely used as a multipurpose fire-extinguishing agent. Serious concerns, however, exist about the risk of depletion and the increasing cost of phosphate rock [2]; hence, new fire-extinguishing agents should be phosphate-free materials. Needless to say, unlike halogenated hydrocarbon fire suppressants such as Halon 1301 (bromotrifluoromethane) and Halon 2402 (dibromotetrafluoroethane), new agents are required to have zero ozone depletion potential [3, 4]. Fine water mist with or without additive(s) is a prime candidate for a new fire-extinguishing agent because of its environmentally friendly, inexpensive, and high-performance characteristics [5]. Additives are used to further enhance the fire suppression efficiency and typically include a surfactant [6, 7], alkali metal salts [8], and transition metal salts [9]. A performance-enhancing agent reduces the amount of suppressant required to extinguish a flame, perhaps resulting in preventing damages due to water.

Transition metal compounds generally have a high ability to extinguish a flame. For instance, iron pentacarbonyl is up to two orders of magnitude more effective than Halon 1301 [10]. However,

iron pentacarbonyl is highly toxic, and the use of this material as a fire-extinguishing agent is therefore very limited. In general, fire suppression applications require the suppressants to have low toxicity and cost and be noncorrosive to fire-extinguishing equipment. Of all the transition-metal compounds, ferrocene (illustrated in Fig. 2a) has drawn attention because of its high suppression capability and low toxicity; several researchers in related fields experimentally demonstrated that ferrocene and its derivatives are good flame inhibitors [11] and flame retardants [12]. For instance, Linteris et al. numerically and experimentally demonstrated the high flame inhibition efficiency of ferrocene vapor [13], and Mehdipour-Ataei and co-workers reported a good flame retardancy for poly(amide ether amide)s having ferrocene moieties [14]. In addition to the good inhibition efficiency of ferrocene, an advantage of using ferrocene is that iron is an abundant element. However, when ferrocene is employed as an additive in water, it has two distinct disadvantages: water insolubility and a decrease in the extinguishing efficiency at higher ferrocene fractions. The former means that it is difficult to use lipophilic ferrocene (as is) as an additive in water. The latter shows that the fire suppression ability of a ferrocene dispersion depends on its concentration [13, 15], implying that the amount of ferrocene added to a flame must be carefully controlled when using ferrocene as an additive. To solve these issues, Koshiba and co-workers [16] recently proposed a novel water-based suppressant containing ferrocene: an aqueous dispersion of ferrocene powder. Such an approach would offer the advantage of easy preparation of dispersions containing an

optimum ferrocene concentration. The earlier studies mainly demonstrated that (i) the extinguishing efficiencies of aqueous ferrocene dispersions are maximized at a ferrocene concentration of approximately 100 ppm (i.e., the fire-extinguishing capability of ferrocene dispersions is also fraction dependent) and that (ii) the extinguishing capability is positively correlated with the dispersibility of ferrocene dispersions. Unfortunately, however, only a few expensive gemini surfactants have been employed. In addition, the corrosive properties of ferrocene dispersions were not investigated. The suppression ability of ferrocene dispersions containing general-purpose and commercially available surfactants and the corrosive properties of such ferrocene dispersions must be investigated.

The present paper describes the fire-extinguishing properties of aqueous ferrocene dispersions containing commercially available and inexpensive nonionic surfactants: Triton X-100 (hereafter referred to as TX), Noigen TDS-80 (NT), Tween 60 (T60, also known as Polysorbate 60), and Tween 80 (T80, also known as Polysorbate 80). The influences of the ferrocene particle size and the surfactant used on the ability of the dispersions to extinguish fires are addressed. Furthermore, the corrosive properties of ferrocene dispersions were studied.

2. Material and Methods

2.1 Chemicals and Materials

Ferrocene was of reagent grade (>98.0%, Wako Pure Chem. Ind. Ltd, Japan). Dry n-heptane (purity: >99.9%, Kanto Chem. Co. Inc., Japan) and deionized water (<1 μS cm^{-1}) were used. As stated above, four commercially available nonionic surfactants (i.e., TX, NT, T60, and T80) were used to disperse ferrocene in water. The chemical structures of TX, NT, T60, and T80 are depicted in Fig. 2b–d. These surfactants are widely used in bio-, food, agricultural, and organic chemistry [17–21]; for instance, a feature of NT is its high biodegradability. Ferrocene and the four surfactants were used as received, without further purification.

Cold-rolled steel plates (also known as SPCC [22], C $\leq$0.15%, Mn $\leq$0.60%, P $\leq$0.100%, and S $\leq$0.050%) with a width of 50 mm, a length of 50 mm, and a thickness of 2 mm were obtained from a fire-extinguisher manufacturer in Japan. SPCC steel is commonly used as the material for fire-extinguisher vessels. In commercial use, the inside wall of the vessel is coated with an epoxy resin; however, the vessel component is not completely covered. From this perspective, SPCC plates without any coating were employed to simply evaluate the corrosion behavior of the aqueous ferrocene dispersions.

2.2 Sample Preparation

Crystalline ferrocene was ball-milled with water at 1,000 rpm for 3 h in an alumina pot using ϕ 3-mm alumina balls or ground in an agate mortar to yield three micron-sized ferrocene samples

(F1–F3) with different particle size distributions. Crystalline ferrocene is light orange in color, while

the micron-sized ferrocene powders were light yellow. Table 1 lists the milling conditions. The

particle size distributions of these samples were measured by a laser diffraction particle size analyzer

(LMS-2000e, Seishin Enterprise Co., Ltd., Japan). As shown in Fig. 3a, the particle size analysis of

the F1 sample gave d_{50} value of 16.9 μm. For the F2 sample, the values of d_{50} were determined to be

30.9 μm (see Fig. 3b), and d_{50} value for the F3 sample were measured as 42.6 μm (see Fig. 3c). The

Rosin–Rammler (R–R) equation, which is used to describe the particle size distribution of crushed

brittle powders [23, 24], is as follows:

$$\ln\left[-\ln\left(\frac{P(X > x)}{100}\right)\right] = \beta(\ln x - \ln\alpha) \quad (1)$$

where x is the ferrocene particle diameter, $P(X > x)$ represents the cumulative percentage of oversize

particles, α is a size parameter (also known as the R–R geometric mean length), and β is a

distribution parameter. As the value of β decreases, the distribution becomes wider. The plots of

$\ln(-\ln(P(X > x)/100))$ versus $\log(x)$ provided β values of 1.28, 1.35, and 2.00 for the F1, F2, and F3

samples, respectively.

A sample of the milled ferrocene was added to an aqueous solution of each surfactant. For each

experiment in this study, the ferrocene concentration was set to 100 ppm on a mass/mass basis and

the surfactant concentration was fixed at twice the critical micelle concentration (CMC) to permit the

formation of micelles in the solution while reducing the influence of the concentrated surfactants

themselves on the suppression efficiency. The CMC values of the surfactants were measured using

the du Noüy ring method [25]. Ultrasonication (43 kHz) for 20 min at 50 °C readily allowed the

preparation of the aqueous ferrocene dispersions. It should be noted here that the dispersions must be

prepared below the cloud points of the surfactants (i.e., the point at which phase separation initiates).

Prior to the dispersion experiments, we confirmed that the cloud points of TX, NT, T60, and T80

were greater than 50 °C. The determination of these cloud points followed a standard method [26].

2.3 Characterization Methods

2.3.1   Visual Observation and Nephelometric Analysis

A visual observation and nephelometric measurement typically provide qualitative and

quantitative information, respectively, regarding the dispersibility. Turbidity is known to be a

function of dispersed particle concentration [27]; turbidity has a positive correlation with the particle

concentration. The nephelometric technique is widely applied to evaluate the dispersibility and

stability of dispersions (e.g., emulsions, suspensions) because the method is simple and rapid [28].

To permit visual observations, 100 mL of the ferrocene dispersions was poured into test tubes 22 mm

in diameter and 200 mm in length. Nephelometric analysis using a turbidimeter (2100Q, Hach Co.,

USA) was conducted to quantitatively evaluate the dispersibility of each dispersion. The turbidity

measurements were sequentially repeated 12 times for each sample, and the values were then

averaged. Turbidity was determined from the ratio of 90° scattered light signals to transmitted light

signals, since ferrocene's color itself strongly affects the turbidity. Both the visual observations and

turbidity measurements were performed at room temperature.

2.3.2 Suppression Experiments

The suppression trials were performed using the experimental apparatus illustrated in Fig. 4a,

which was designed to simply compare the extinguishing capabilities of the ferrocene dispersions.

80 mL of *n*-heptane was poured into a pan with a diameter of 83 mm. Following ignition, the fires

were allowed to burn freely until a quasi-steady state was reached. A nozzle placed 600 mm above

the pan was then activated. The flow rate and spray angle were set to 250 mL min^{-1} and 60°,

respectively. Mean extinguishing times (τ) for each dispersion were determined following 10 repeat

experiments.

Prior to the suppression trials, the spray characteristics were evaluated. The spray pattern was

similar to a full-cone. In this study, the Sauter mean diameter (D_{32}, Eq. 2) of the mist droplets were

measured by the immersion technique [29],

$$D_{32} = \frac{\sum N_i D_i^3}{\sum N_i D_i^2}. \qquad (2)$$

where N_i is the measured number of droplets with diameter D_i. Droplets collected into silicone oil positioned 600 mm below the nozzle were inspected using a digital microscope (DMI 3000B, Leica, Germany). As a result, D_{32} and D_{90} were found to be 313 and 416 μm, respectively. An advantage of the immersion method lies in the direct observation of gathered droplets. Note that Hurlburt pointed out that the droplet diameter may depend on the droplet measuring technique, such as laser diffraction, phase Doppler, and freezing methods [29]. Regardless of this, the diameter of the ferrocene powder used in this study was an order of magnitude smaller than the mist droplets, thereby indicating that the ferrocene particles are contained within the water droplets.

The viscosities (η) of the ferrocene dispersions containing nonionic surfactants were determined at 19 °C using a viscometer (SV-10, A&D Company, Japan) according to a standard test method [30].

2.3.3   Corrosion Tests

The corrosion experiments were conducted using the experimental setup depicted in Fig. 4b. Prior to the corrosion experiments, the SPCC plate was thoroughly rinsed with ethanol and then dried. An acrylic tube with a 45 mm diameter and 100 mm height was attached to the plate with an adhesive. The corrosion trials were performed under a nitrogen atmosphere, as nitrogen is commonly

used in Japan for stored-pressure fire extinguishers. In this experiment, the ferrocene dispersions containing TX were tested, as they exhibited superior fire-suppression abilities compared to the other ferrocene dispersions tested in this study (as noted later). 100 mL of the aqueous TX solution, the TX-containing F1 ferrocene dispersions, and deionized water was degassed with nitrogen (>99.99%) for 2 h prior to the measurements of potential. They were then poured into the acrylic tube; the area of the specimen plate exposed was 15.9 cm^2. The corrosion potentials of the specimens were measured using a high-input-impedance electrometer (PS-14, Toho Technical Research, Japan) at room temperature. To avoid eluting ions from the reference electrode (Ag/AgCl, sat. KCl), it was immersed in the test solutions only during the potential measurements. After 14 days, the surfaces of the specimen plates were rinsed with ethanol and then inspected with a laser scanning microscope (VR-3000, Keyence, Japan) to evaluate the corrosion behavior of the mixtures.

3. Results

3.1 Dispersibility of the Ferrocene Dispersions

To visually observe the sedimentation behavior of the ferrocene particles at room temperature, the ferrocene dispersions were poured into long test tubes. At 0 min, the dispersions containing F1 ferrocene had a cloudy yellow appearance, while the F3 ferrocene dispersions immediately produced a small amount of yellow precipitate at the bottom of the test tubes. These results imply that

dispersibility had a negative relationship with the ferrocene particle size. After 240 min, the F1 ferrocene dispersions were somewhat yellow and turbid, while most of the ferrocene particles were observed at the bottoms of the test tubes for the F3 ferrocene dispersions.

Fig. 5 depicts the turbidity of the dispersions as a function of time. The variations in the turbidity of the dispersions containing F1, F2, and F3 ferrocene are shown in Fig. 5a, 5b, and 5c, respectively. By comparing the turbidity among the surfactants, it is clear that the surfactants ranked in the following order in terms of their dispersibility: TX > NT > T60 > T80. These figures also show that the turbidity of the ferrocene dispersions increased in the order F1 > F2 > F3. The results obtained from the nephelometric measurement are therefore in good agreement with the visual observations described above.

3.2 Fire Suppression Efficiency of the Ferrocene Dispersions

In general, surfactant concentration has a remarkable influence on fire suppression efficiency [6]. However, the present study confirmed that pure water mist, either with or without a surfactant (i.e., TX, NT, T60, and T80) at twice their CMC value, did not extinguish the pool fire, thus enabling a direct comparison of the fire suppression efficiency among the ferrocene dispersions. This is probably because the concentrations of surfactants used in this study were too low to permit fire suppression activity (TX: 0.028 wt%, NT: 0.011 wt%, T60: 0.005 wt%, and T80: 0.002 wt%).

The extinguishing times of the ferrocene dispersions are shown in Fig. 6; the extinguishing time

of a conventional wet chemical containing 45-wt% potassium carbonate is also depicted for

reference (τ = 12.9 s [16]). With the exception of dispersion containing TX, the F2 and F3 ferrocene

dispersions containing the nonionic surfactants exhibited significantly longer extinguishing times

than the wet chemical agent, whereas the F1 ferrocene dispersions tested in this study had better

suppression abilities: τ = 5.5 s for the F1 ferrocene dispersion containing TX, τ = 6.1 s for the F1

ferrocene dispersion containing NT, τ = 11.5 s for the F1 ferrocene dispersion containing T60, and τ

= 8.9 s for the F1 ferrocene dispersion containing T80. Interestingly, the ferrocene dispersions

containing TX were effective at suppressing pool fires, even if F2 and F3 ferrocene powders were

employed (τ = 6.5 s for the F2 ferrocene dispersion containing TX and τ = 6.8 s for the F3 ferrocene

dispersion containing TX). The ferrocene dispersions tested in this study were ranked in the

following order in terms of their suppression capabilities: F1 ferrocene dispersions > F2 ferrocene

dispersions ≥ F3 ferrocene dispersions.

3.3 Corrosion Behavior

Fig. 7 depicts the corrosion potentials for the three types of solutions as a function of time. In the

initial stages, there were significant differences in the potentials of the solutions studied: pure water,

an aqueous solution of TX, and the F1 ferrocene dispersions containing TX. This is because an oxide

layer formed in air dissolves, which is not due to ferrocene itself but due to the surface conditions of

the specimen plates. The corrosion potentials eventually reached a plateau after 4 days, and the

potentials after 14 days were −489, −459, and −471 mV vs. SHE for pure water, the aqueous solution

of TX, and the F1 ferrocene dispersions containing TX, respectively. Surfactants typically behave as

corrosion inhibitors [31], which hampers metal dissolution. However, no significant difference was

observed in terms of the potentials of the pure water and the aqueous TX solution after 14 days. This

is probably because the surfactant concentrations used in this study were too low to reduce corrosion

rates. The potentials should decrease if ferrocene itself acts as a one-electron reducing agent

according to Eq. (3) [32]; however, the corrosion trials also revealed no significant difference in the

potentials of the aqueous TX solution and the F1 ferrocene dispersions containing TX after 14 days.

$$Fe(C_5H_5)_2 \rightarrow Fe(C_5H_5)_2^+ + e^- \qquad (3)$$

Fig. 8 shows the Pourbaix Diagram for iron-water systems at 298 K; the corrosion potential of

each solution after 14 days plotted as a function of the pH is superimposed on the diagram. All the

plots in the diagram were in the corrosion region. We confirmed that no clear pitting corrosion was

observed after 14 days immersion for any of the three specimens. These results clearly demonstrated

that the specimens tested were uniformly corroded. In general, pitting corrosion may cause more

14

severe damage than uniform corrosion [33]. The corrosion risks associated with the use of

epoxy-coated SPCC steel, which is used for the inside walls of fire-extinguishers, are negligible

under standard operating conditions; thus, it is probable that ferrocene dispersions containing

nonionic surfactants will also not present a corrosion risk.

4. Discussion

The main objectives of the present study were to investigate (i) the effects of ferrocene particle

size and surfactant type on fire-extinguishing capability and (ii) the corrosive properties of ferrocene

dispersions containing the general-purpose nonionic surfactants: TX, NT, T60, and T80. The

corrosion experiments described above revealed that ferrocene dispersions containing nonionic

surfactants did not exhibit corrosive properties. Hence, hereafter, only the extinguishing capability

will be addressed.

For statistically testing the differences in the extinguishing times among the ferrocene

dispersions containing nonionic surfactants, a two-way analysis of variance (two-way ANOVA)

followed by a *post hoc* analysis (Tukey's honest significant differences (HSD) test [34]) was

conducted. Before performing the ANOVA tests, all data were log-transformed to correct for

heteroscedasticity and non-normality; homoscedasticity was assessed with the Levene's and

Bartlett's tests, and normality was confirmed using the Kolmogorov–Smirnov test [35]. In this study,

a significance level of 0.05 was used.

A two-way ANOVA confirmed that the interaction between the nonionic surfactant and the ferrocene particle size was not statistically significant ($F = 0.256$, $p = 0.96$). A simple main effects analysis revealed that the type of nonionic surfactant ($F = 13.053$, $p < 0.001$) and the ferrocene diameter ($F = 11.612$, $p < 0.001$) were significant factors.

A Tukey's HSD multiple comparison revealed significant differences in the extinguishing times between ferrocene–TX and ferrocene–NT dispersions ($p < 0.05$), ferrocene–TX and ferrocene–T60 dispersions ($p < 0.001$), ferrocene–TX and ferrocene–T80 dispersions ($p < 0.001$), and ferrocene–NT and ferrocene–T60 dispersions ($p < 0.05$) (see Table 2). This result means that the extinguishing capabilities decreased in the following order: ferrocene dispersions containing TX > ferrocene dispersions containing NT > ferrocene dispersions containing T60 ≈ ferrocene dispersions containing T80. Fig. 9 shows the variations in the extinguishing times as a function of the corresponding initial turbidity of the ferrocene dispersions containing nonionic surfactants, with the exception of dispersions containing TX. These plots were approximately linear with a high coefficient of determination (0.80), which demonstrates that the suppression efficiency is positively correlated with the dispersibility of the ferrocene nonionic surfactant dispersion systems; the result obtained from the present study was in good agreement with that reported in the literature [36]. In an iron-catalyzed radical recombination mechanism involving H, OH, and O, the radical-recombination

16

efficiency markedly depends on the concentrations of active iron-inhibiting species (e.g., FeO, $Fe(OH)_2$, FeOH, and Fe) [37]. The presence of iron-inhibiting species at extremely high concentrations triggers their agglomeration and condensation, which leads to a reduction in the suppression efficiency [37]. The fact that ferrocene at its optimum concentration must be homogeneously added into a flame agrees well with the result that ferrocene dispersions with poor dispersibilities exhibit high suppression capabilities, even if ferrocene dispersions have the same ferrocene concentration, as shown in Fig. 9. Remarkably, however, even the TX-containing ferrocene dispersions that showed poor dispersibilities exhibited high fire suppression abilities. The suppression efficiency is influenced not only by the presence of an additive(s) but also by the spray characteristics (e.g., droplet size) [38]. The droplet size is generally dominated by surface tension, viscosity, specific gravity, and pressure. In this study, the pressure was kept constant, and there were no significant differences in the other three parameters between the ferrocene dispersions since the concentrations of the surfactants and ferrocene were extremely low (100 ppm of ferrocene and twice CMC of the surfactants). For example, η = 1.05, 1.06, 1.06, 1.06, and 1.07 mPa·s for the ferrocene dispersions containing TX, NT, T60, and T80, and pure water, respectively. Hence, further research is needed to explain the anomalous behavior of ferrocene dispersions containing TX.

A Tukey's HSD multiple comparison also revealed significant differences in the extinguishing times among F1, F2, and F3 ferrocene dispersions. As seen in Table 3, F1 ferrocene dispersions had

significantly higher extinguishing abilities than F2 and F3 ferrocene dispersions. This result is

entirely consistent with the finding that the extinguishing capability is negatively correlated with the

particle size of the suppressant [39, 40].

5. Conclusions

In this paper, the extinguishing capabilities and corrosion properties of ferrocene dispersions

containing general-purpose nonionic surfactants were investigated, leading to the following

conclusions:

- Suppression experiments and two-way ANOVA tests revealed that aqueous dispersions

  containing smaller ferrocene particles exhibited higher extinguishing capabilities. In particular,

  when prepared with F1 ferrocene ($d_{50} = 16.9$ μm), ferrocene dispersions have significantly

  shorter extinguishing times than a wet chemical. Suppression trials and nephelometric

  measurements also demonstrated that for the ferrocene dispersions containing such nonionic

  surfactants, the suppression ability of the ferrocene dispersions was positively correlated to their

  dispersibilities (i.e., their initial turbidities).

- Corrosion experiments clearly demonstrated that no pitting corrosion of SPCC steels are

  observed, thus indicating that ferrocene dispersions containing TX do not pose a serious

corrosion problem.

The experimental results given in the present study open the way for the development of new, effective fire suppressants containing ferrocene.

Acknowledgments

References

1. Fire and Disaster Management Agency (2014) Fire statistics in Japan in 2014. <http://www.fdma.go.jp/neuter/topics/houdou/h27/04/270413_houdou_1.pdf> (in Japanese) Accessed 10 February 2016.

2. D. Cordell, T.-S.S. Neset, Phosphorus vulnerability: a qualitative framework for assessing the vulnerability of national and regional food systems to the multidimensional stressors of

phosphorus scarcity, Glob. Environ. Change 24 (2014) 108–122.

3. S.E. Hodges, S.J. McCormick, Fire extinguishing agents for protection of occupied spaces in military ground vehicles, Fire Technol. 49 (2013) 379–394.

4. J.A. Senecal, Halon replacement chemicals: perspectives on the alternatives, Fire Technol. 28 (1992) 332–344.

5. K.C. Adiga, R.F. Hatcher Jr, R.S. Sheinson, F.W. Williams, S. Ayers, A computational and experimental study of ultra fine water mist as a total flooding agent, Fire Saf. J. 42 (2007) 150–160.

6. G. LeFort, A.W. Marshall, M. Pabon, Evaluation of surfactant enhanced water mist performance, Fire Technol. 45 (2009) 341–354.

7. Z. Xiaomeng, L. Guangxuan, C. Bo, Improvement of water mist's fire-extinguishing efficiency with MC additive, Fire Saf. J. 41 (2006) 39–45.

8. A.G. Shmakov, O.P. Korobeinichev, V.M. Shvartsberg, S.A. Yakimov, D.A. Knyazkov, V.F. Komarov, G.V. Sakovich, Testing ogranophosphorus, organofluorine, and metal-containing compounds and solid-propellant gas-generating compositions doped with phosphorus-containing additives as effective fire suppressant, Combust. Explos. 42 (2006) 678–687.

9. O.P. Korobeinichev, A.G. Shmakov, V.M. Shvartsberg, A.A. Chernov, S.A. Yakimov, K.P. Koutsenogii, V.I. Makarov, Fire suppression by low-volatile chemically active fire suppressants

using aerosol, Fire Saf. J. 51 (2012) 102–109.

10. D. Reinelt, G.T. Linteris, Experimental study of the inhibition of premixed and diffusion flames by iron pentacarbonyl, Proc. Symp. (Int.) Combust. 26 (1996) 1421–1428.

11. Y. Koshiba, S. Agata, T. Takahashi, H. Ohtani, Direct comparison of the flame inhibition efficiency of transition metals using metallocenes. Fire Saf. J. 73 (2015) 48–54.

12. N. Najafi-Mohajeri, G.L. Nelson, R. Benrashid, Synthesis and properties of new ferrocene-modified urethane block copolymers, J. Appl. Polym. Sci.76 (2000) 1847–1856.

13. G.T. Linteris, M.D. Rumminger, V. Babushok, W. Tsang, Flame inhibition by ferrocene and blends of inert and catalytic agent, Proc. Combust. Inst. 28 (2000) 2965–2972.

14. S. Mehdipour-Ataei, A. Tadjarodi, S. Babanzadeh, Novel ferrocene modified poly(amide ether amide)s and investigation of physical and thermal properties. Eur. Polym. J. 43 (2007) 498–506.

15. Y. Koshiba, Y. Takahashi, H. Ohtani, Flame suppression ability of metallocenes (nickelocene, cobaltocene, ferrocene, manganocene, and chromocene), Fire Saf. J. 51 (2012) 10–17.

16. Y. Koshiba, K. Iida, H. Ohtani, Fire extinguishing properties of novel ferrocene/surfynol 465 dispersions, Fire Saf. J. 72 (2015) 1–6.

17. M. Hirohama, A. Kumar, I. Fukuda, S. Matsuoka, Y. Igarashi, H. Saitoh, M. Takagi, K. Shin-ya, K. Honda, Y. Kondoh, T. Saito, Y. Nakao, H. Osada, K.Y.J. Zhang, M. Yoshida, A. Ito, Spectomycin B1 as a novel SUMOylation Inhibitor that directly binds to SUMO E2, ACS Chem.

Biol. 8 (2013) 2635–2642.

18. K. Numata, Y. Motoda, S. Watanabe, T. Osanai, T. Kigawa, Co-expression of two polyhydroxyalkanoate synthase subunits from Synechocystis sp. PCC 6803 by cell-free synthesis and their specific activity for polymerization of 3-hydroxybutyryl-coenzyme A, Biochem. 54 (2015) 1401–1407.

19. B.K. Amos, R.C. Daprato, J.B. Hughes, K.D. Pennell, F.E. Löffler, Effects of the nonionic surfactant tween 80 on microbial reductive dechlorination of chlorinated ethenes, Environ. Sci. Technol. 41 (2007) 1710–1716.

20. K. Niikura, E.V. Anslyn, Triton X-100 enhances ion-pair-driven molecular recognition in aqueous media. Further work on a chemosensor for inositol trisphosphate, J. Org. Chem. 68 (2003) 10156–10157.

21. S. Sharma, S. Kori, A. Parmar, Surfactant mediated extraction of total phenolic contents (TPC) and antioxidants from fruits juices, Food Chem. 185 (2015) 284–288.

22. JIS G3141, Cold-reduced carbon steel sheet and strip. in: JIS Handbook, Tokyo, 2012.

23. S.E. Allaire, L.-E. Parent, Size guide number and Rosin–Rammler approaches to describe particle size distribution of granular organic-based fertilizer, Biosyst. Eng. 86 (2003) 503–509.

24. Y. Hairui, M. Wirsum, Y. Guangxi, F.N. Fett, X. Youning, A six-parameter model to predict ash formation in a CFB boiler, Powder Technol. 134 (2003) 117–122.

25. K. Holmberg, B. Jőnsson, B. Kronberg, B. Lindman, Surfactants and polymers in aqueous solution, 2nd ed., John Wiley & Sons, Ltd., Chichester, 2003.

26. ASTM D2024-09, Standard Test Method for Cloud Point of Nonionic Surfactants. vol. 15.04, West Conshohocken, PA, 2013.

27. S.R. Reddy, H.S. Fogler, Emulsion stability: determination from turbidity, J. Colloid Interface Sci. 79 (1981) 101–104.

28. K. Rahn-Chique, A.M. Puertas, M.S. Romero-Cano, C. Rojas, G. Urbina-Villalba, Nanoemulsion stability: experimental evaluation of the flocculation rate from turbidity measurement., Adv. Colloid Interface Sci. 178 (2012) 1–20.

29. E.T. Hurlburt, T.J. Hanratty, Measurement of drop size in horizontal annular flow with the immersion method, Exp. Fluids 32 (2002) 692–699.

30. JIS Z8803, Methods for viscosity measurement of liquid, in: JIS Handbook, Tokyo, 2011.

31. G.I. Ostapenko, P.A. Gloukhov, A.S. Bunev, Investigation of 2-cyclohexenylcyclohexanone as steel corrosion inhibitor and surfactant in hydrochloric acid, Corr. Sci. 82 (2014) 265–270.

32. Y. Yamada, J. Mizutani, M. Kurihara, H. Nishihara, Synthesis of a new bis(ferrocenlyl)ruthenacyclopentatriene compound with a significant inter-metal electronic communication, J. Organomet. Chem. 637–639 (2001) 80–83.

33. M.A. Javed, P.R. Stoddart, S.A. Wade, Corrosion of carbon steel by sulphate reducing bacteria:

Initial attachment and the role of ferrous ions, Corr. Sci. 93 (2015) 48–57.

34. M. Garaud, J. Trapp, S. Devin, C. Cossu-Leguille, S. Pain-Devin, V. Felten, L. Giamberini, Multibiomarker assessment of cerium dioxide nanoparticle (nCeO$_2$) sublethal effects on two freshwater invertebrates, *Dreissena polymorpha and Gammarus roeseli*, Aquat. Toxicol. 158 (2015) 63–74.

35. J. Ekasari, D.R. Rivandi, A.P. Firdausi, E.H. Surawidjaja, M. Zairin Jr., P. Bossier, P. De Schryver, Biofloc technology positively affects Nile tilapia (Oreochromis niloticus) larvae performance, Aquaculture 441 (2015) 72–77.

36. Y. Koshiba, H. Ohtani, Extinguishing pool fires with aqueous ferrocene dispersions containing gemini surfactants, J. Loss Prev. Process Ind. 40 (2016) 10–16.

37. G.T. Linteris, M.D. Rumminger, V.I. Babushok, Catalytic inhibition of laminar flames by transition metal compounds, Prog. Ener. Combust. Sci. 34 (2008) 288–329.

38. P.E. Santangelo, B.C. Jacobs, N. Ren, J.A. Sheffel, M.L. Corn, A.W. Marshall, Suppression effectiveness of water-mist sprays on accelerated wood-crib fires, Fire Saf. J. 70 (2014) 98–111.

39. C.T. Ewing, F.R. Faith, J.B. Romans, C.W. Siegmann, R.J. Ouellette, J.T. Hughes, H.W. Cathart, Extinguishing class B fires with dry chemicals: scaling studies, Fire Technol. 31 (1995) 17–43.

40. C.J. Kibert, D. Dierdorf, Solid particulate aerosol fire suppressants, Fire Technol. 30 (1994). 388–399.

Figure captions

Fig. 1

Trends in fires, deaths, and economic losses from 2009 to 2014 in Japan (adapted from [1]).

Fig. 2

Chemical structures of (a) ferrocene and the nonionic surfactants: (b) Triton X-100 (TX, m = 10), (c)

Noigen TDS-80 (NT, n = 8, R = n-C$_{13}$H$_{27}$), and (d) Tween 60 (T60, w + x + y + z = 20, R =

CO(CH$_2$)$_{16}$CH$_3$) and Tween 80 (T80, w + x + y + z = 20, R = cis-CO(CH$_2$)$_7$CH=CH(CH$_2$)$_7$CH$_3$).

Fig. 3

Particle size distributions of (a) F1 ferrocene, (b) F2 ferrocene, and (c) F3 ferrocene powders.

Fig. 4

Schematic representation of the experimental apparatus used for (a) the suppression tests and (b) the

corrosion tests.

Fig. 5

Turbidities of ferrocene dispersions as a function of time (triangles = dispersions containing TX,

squares = dispersions containing NT, lozenges = dispersions containing T60, and circles = dispersions containing T80. (a) F1 ferrocene, (b) F2 ferrocene, and (c) F3 ferrocene.

Fig. 6

Extinguishing times of the ferrocene dispersions (dark gray bars = F1 ferrocene dispersions, light gray bars = F2 ferrocene dispersions, and striped bars = F3 ferrocene dispersions) and wet chemical containing 45-wt% potassium carbonate. Error bars indicate standard deviations. a: adapted from [16].

Fig. 7

Corrosion potentials of SPCC plates in a nitrogen atmosphere as a function of time; triangles = pure water, squares = aqueous solution of TX, and circles = F1 ferrocene dispersions containing TX.

Fig. 8

Experimental data superimposed onto the Pourbaix Diagram for an iron-water system at 298 K and 10^{-6} mol/kg.

Fig. 9

Extinguishing times of ferrocene dispersions containing nonionic surfactants as a function of their

corresponding initial turbidities. The line depicted is generated using the least squares method.

Table captions

Table 1

Ferrocene milling conditions and parameters of the Rosin–Rammler distribution.

Table 2

p-Values matrix assessing the main effect of the surfactant on the extinguishing time.

Table 3

p-Values matrix assessing the main effect of the ferrocene size on the extinguishing time.

Table 1

Sample	Method	Milling condition	d_{50} (μm) [c]	β [d]
F1	Ball milling	Wet [a], 1000 rpm, 3h	16.9	1.28
F2	Ball milling	Wet [b], 1000 rpm, 3h	30.9	1.35
F3	Agate mortar	Dry	42.6	2.00

a: Ferrocene/water ratio: 3.31, b: ferrocene/water ratio:3.0, c: determined by a laser diffraction particle size analyzer, d: determined by the Rosin Rammler equation.

Table 2

	1	2	3	4
1 Ferrocene dispersions containing TX		0.0172[*]	0.000[**]	0.000[**]
2 Ferrocene dispersions containing NT			0.0363[*]	0.384
3 Ferrocene dispersions containing T60				0.575
4 Ferrocene dispersions containing T80				

*: $p < 0.05$; ** $p < 0.01$

Table 3

	1	2	3
1 F1 ferrocene dispersions		0.001^{**}	0.000^{**}
2 F2 ferrocene dispersions			0.588
3 F3 ferrocene dispersions			

** $p < 0.01$

Figure 1
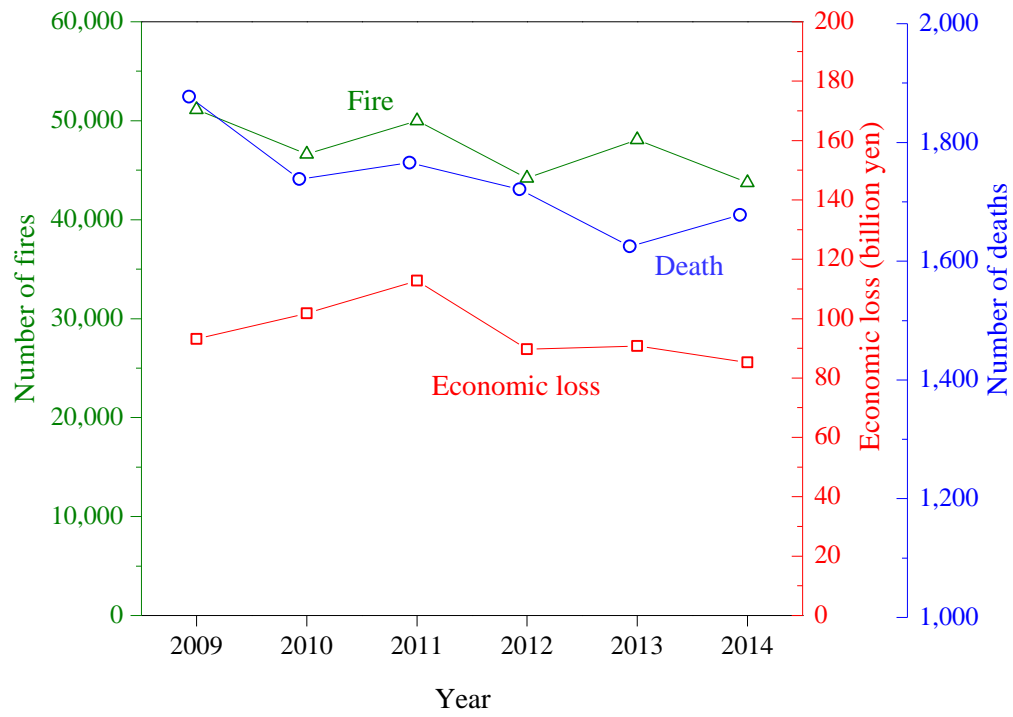
Figure2

a

b

c

d
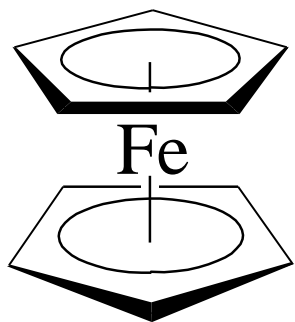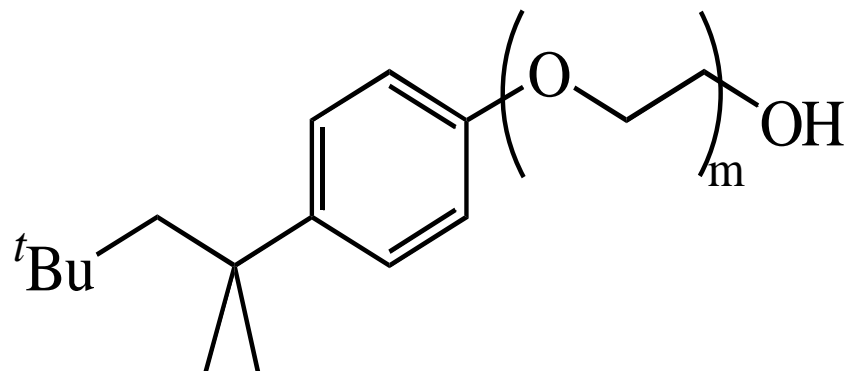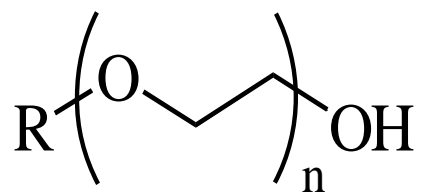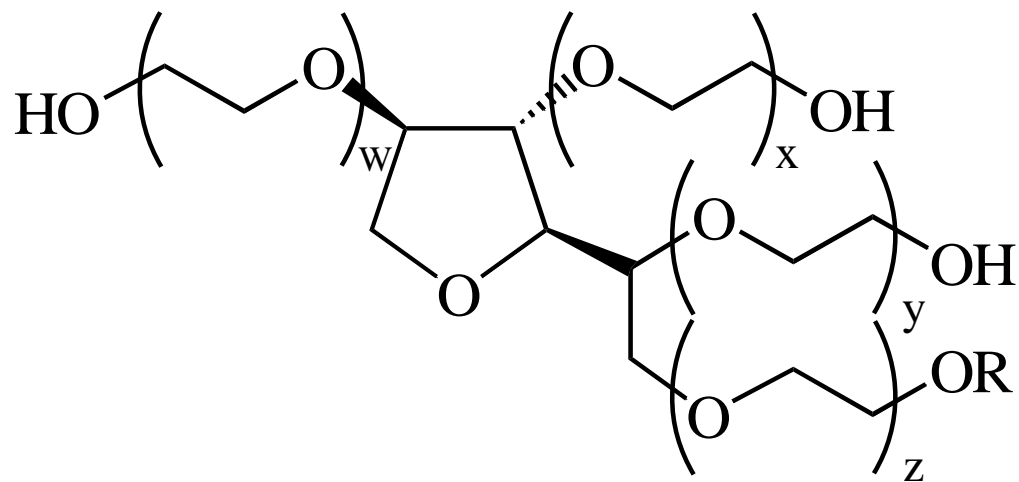
Figure 3
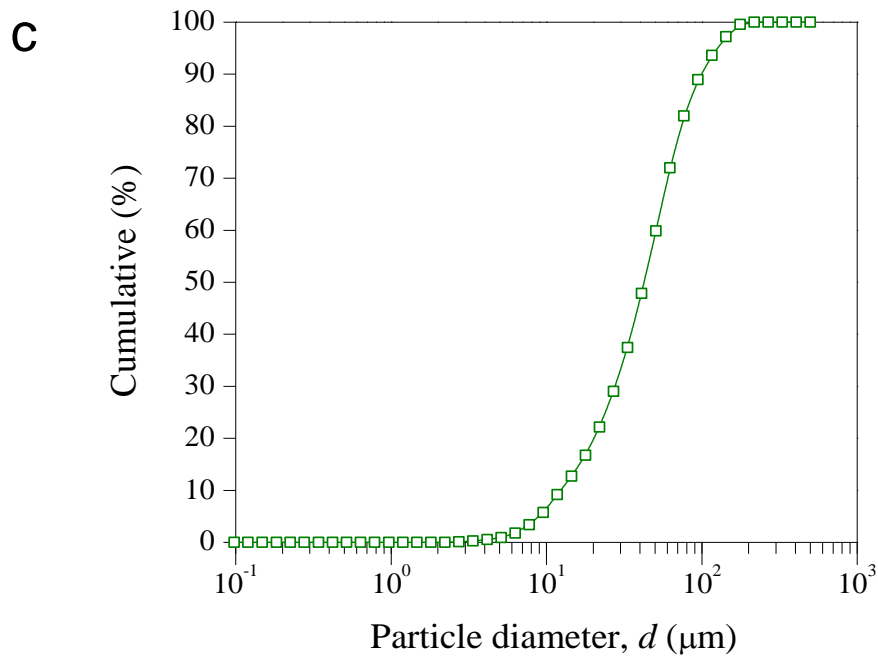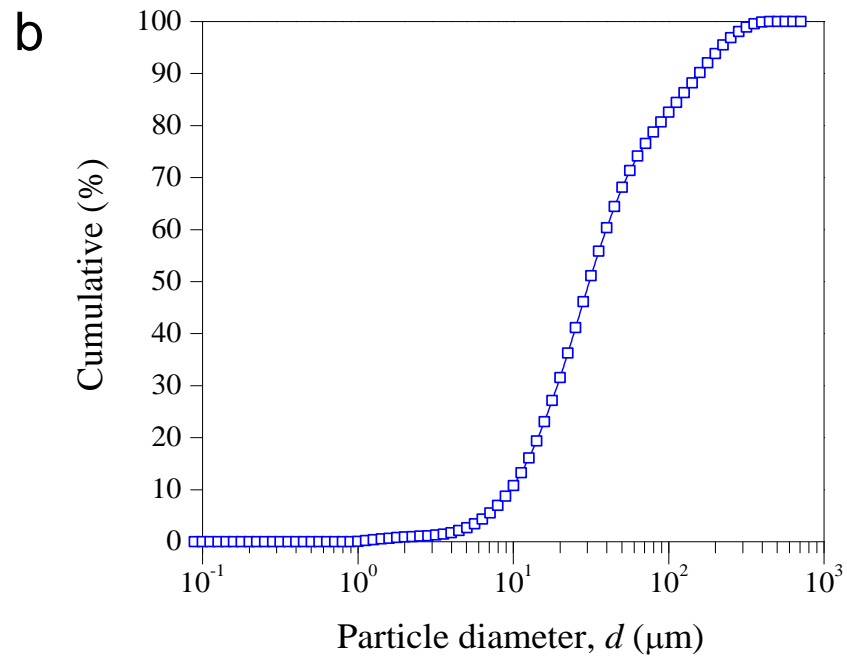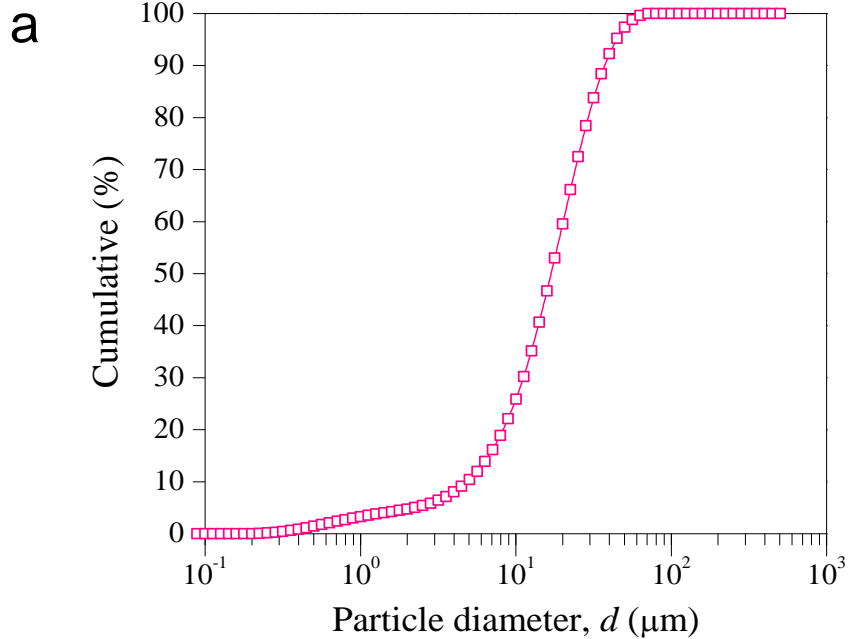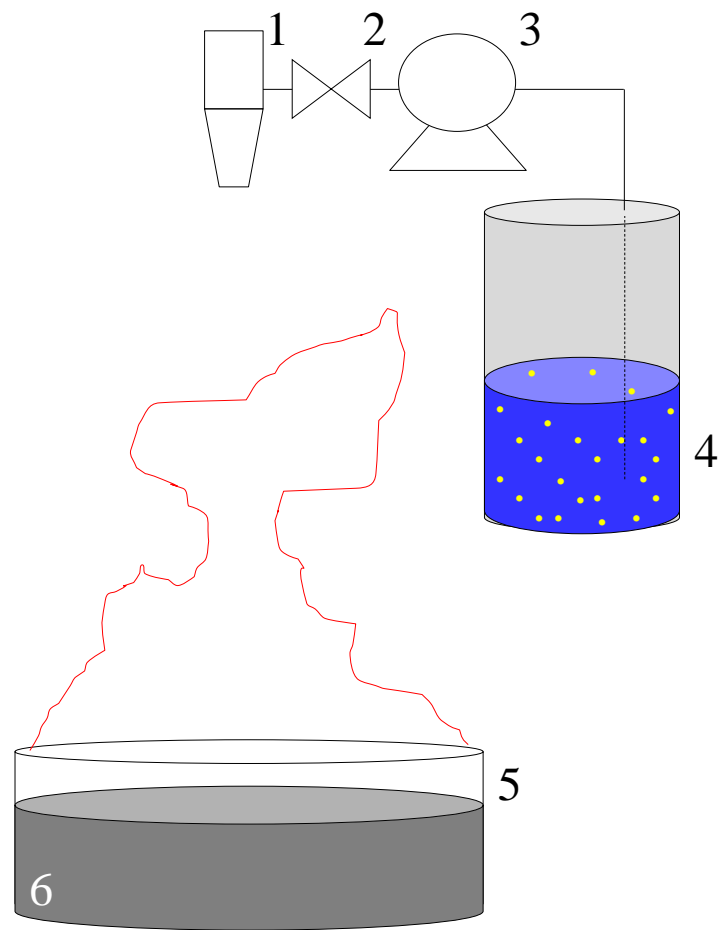
1. nozzle, 2. valve, 3. pump,
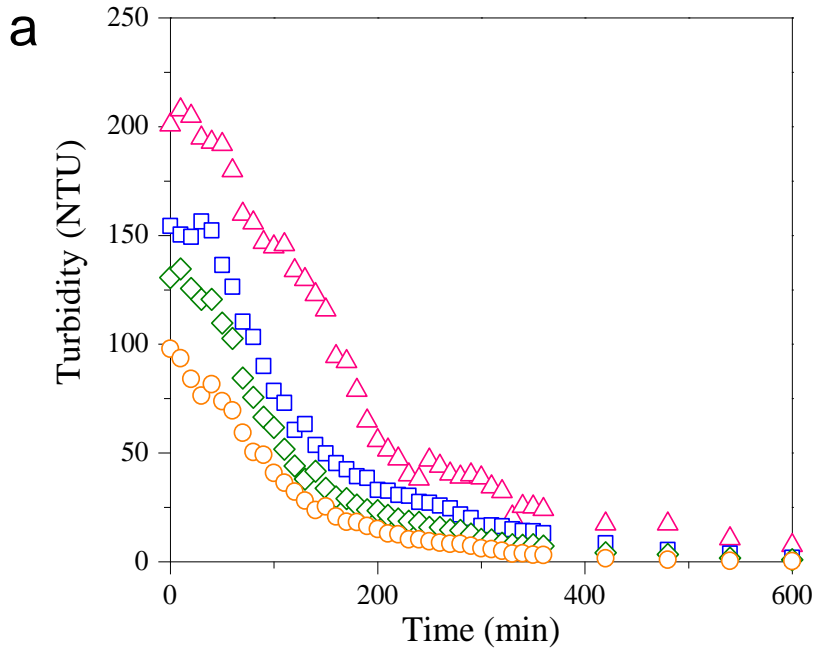4. ferrocene dispersion, 5. pan, 6. n-heptane.

N$_2$ outlet   N$_2$ inlet

Acrylic tube

Aqueous ferrocene dispersion,
aqueous solution of TX, or water

SPCC plate

Figure 5
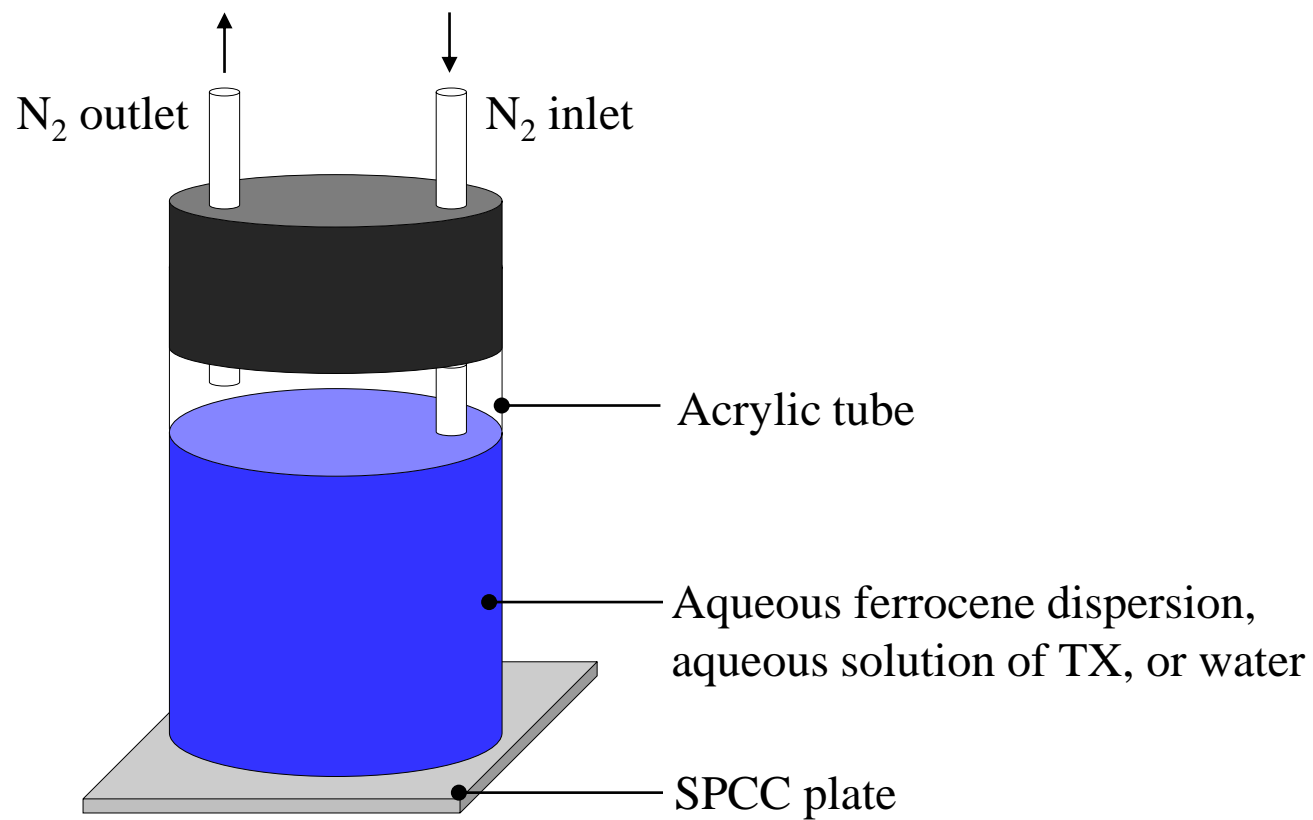
Figure 6
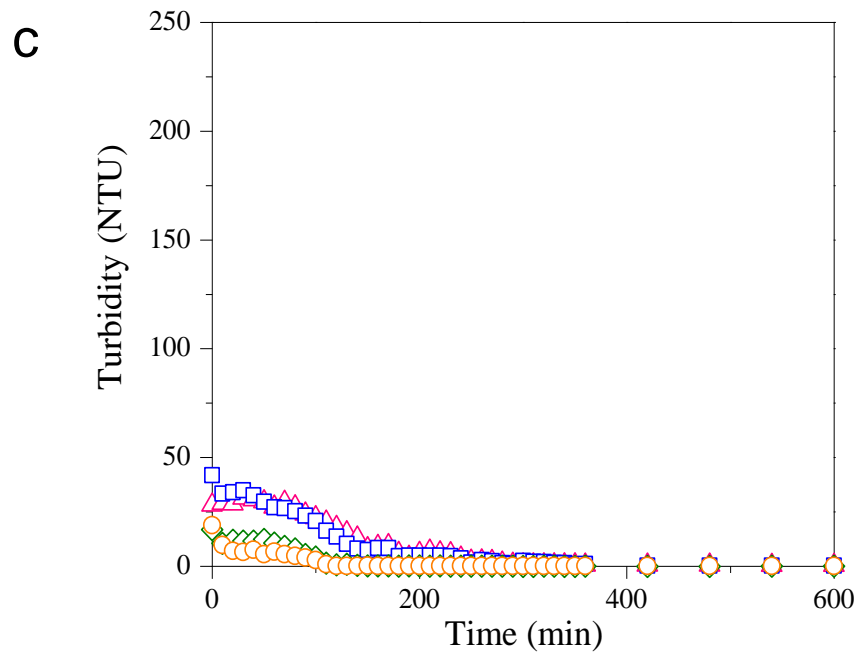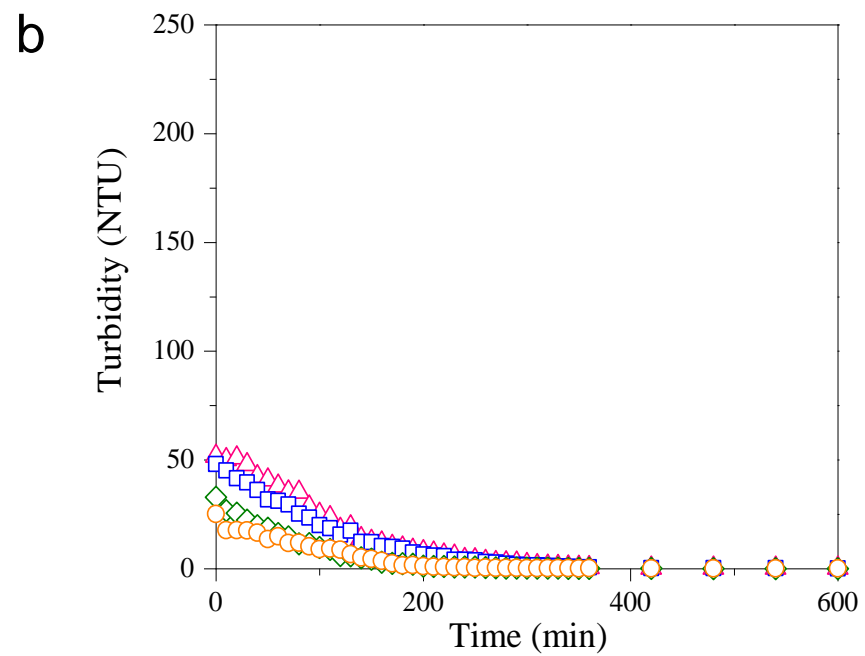
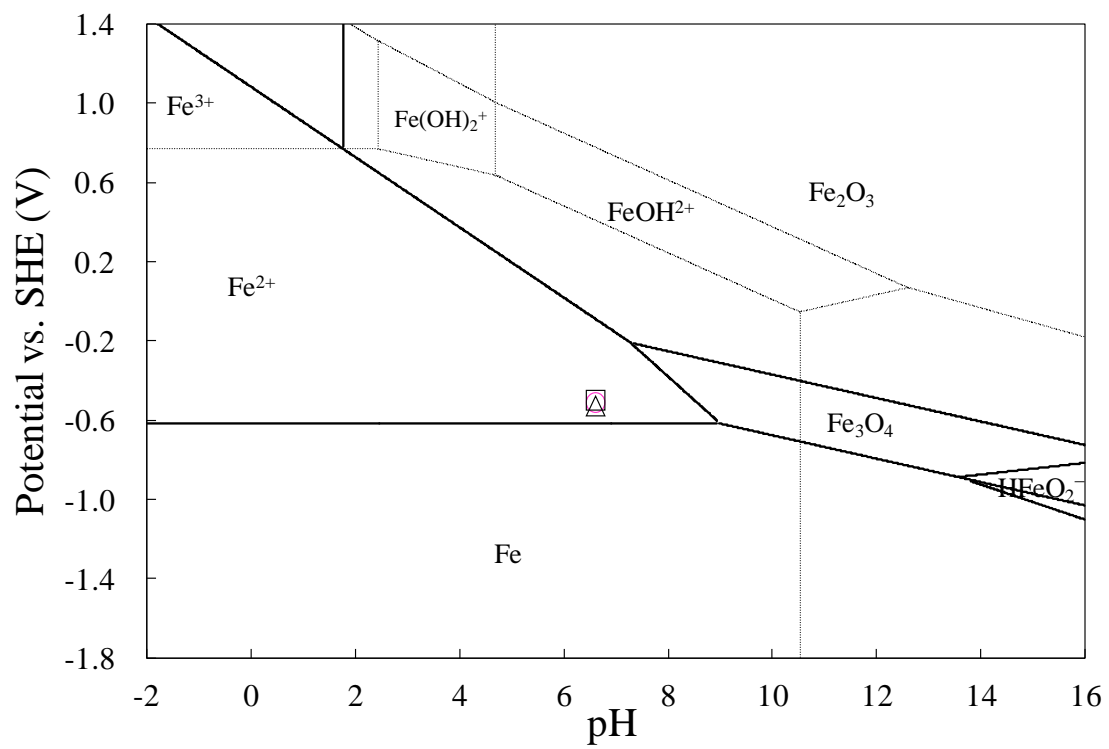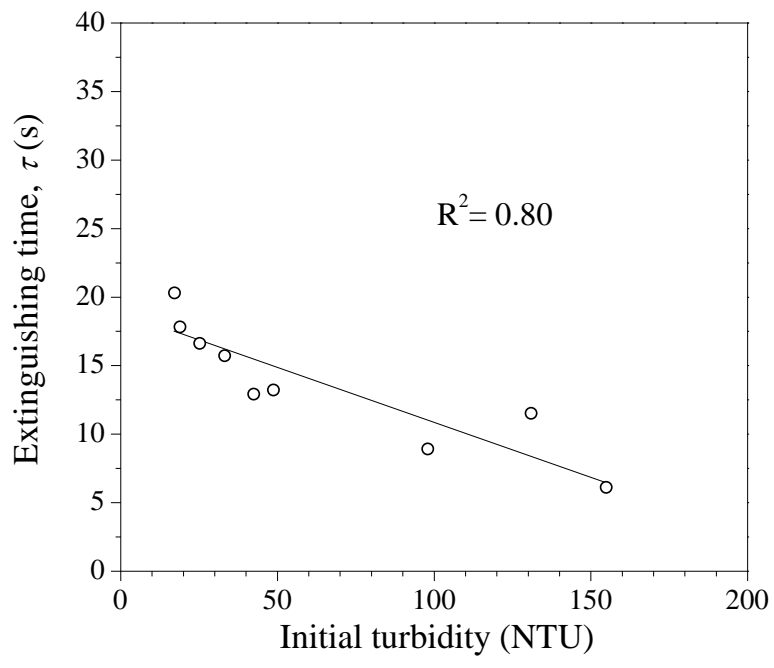Extinguishing time, τ (s)
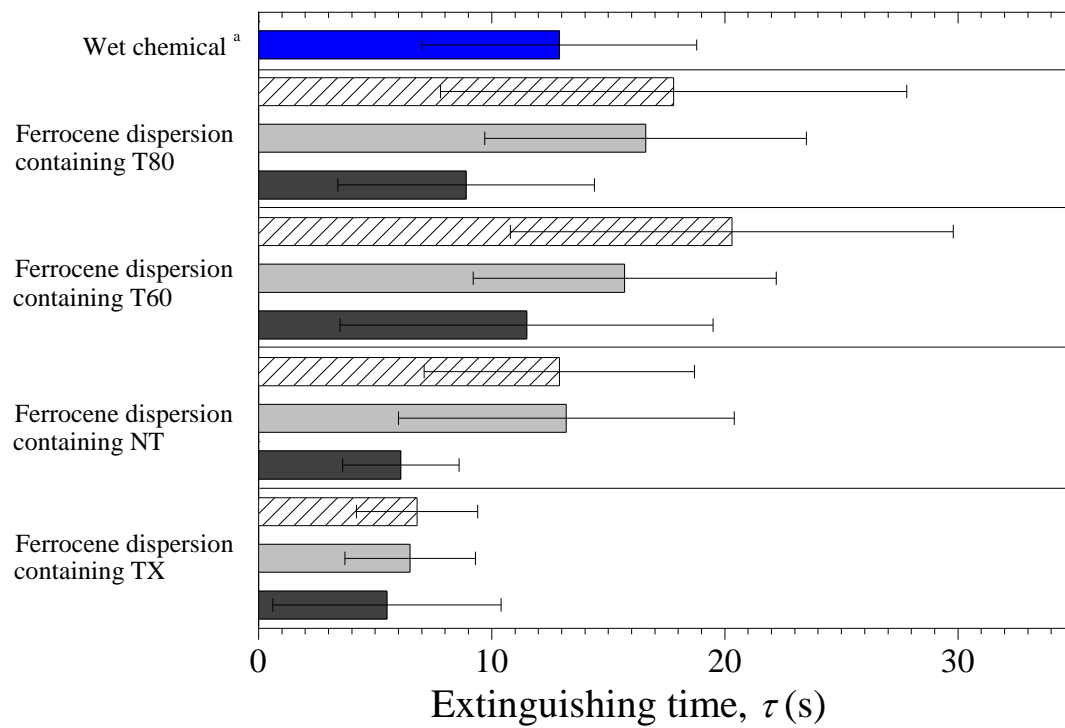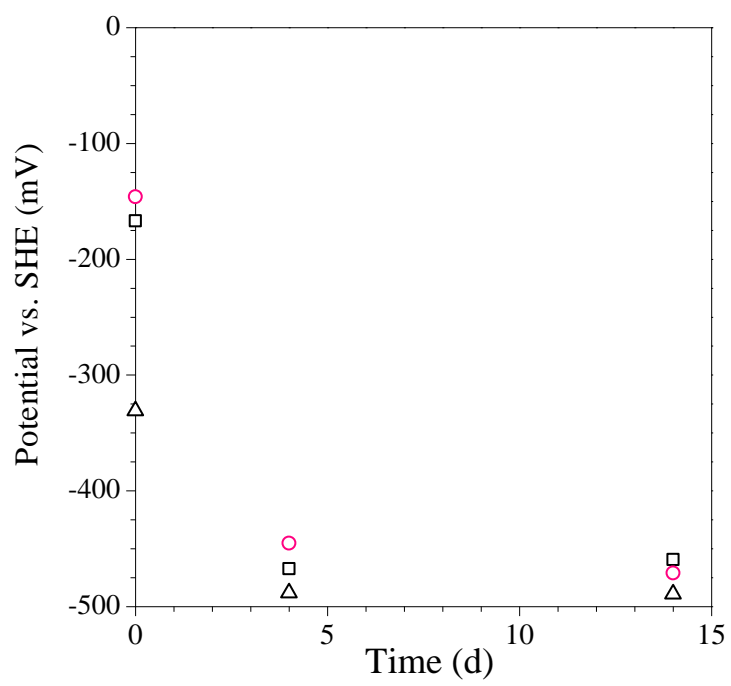
Figure 7

Figure 8

Figure 9

Highlights

- The extinguishing abilities and corrosive properties of ferrocene dispersions are

  investigated.

- The extinguishing capability is negatively correlated with the particle size of ferrocene.

- The extinguishing capabilities decrease in the following order: ferrocene dispersions

  containing TX > ferrocene dispersions containing NT > ferrocene dispersions containing

  T60 ≈ ferrocene dispersions containing T80.

- The ferrocene dispersions containing triton X-100 do not present a corrosion risk.